Biointerface Research in Applied Chemistry
Open-Access Journal (ISSN: 2069-5837)

Article
Volume 16, Issue 2, 2026, 47
https://doi.org/10.33263/BRIAC162.047

A Butyrate Derivative Attenuates the Bruton's Tyrosine Kinase Phosphorylation-Dependent Activation of Calcium Phosphate

Minh Tan Pham[1,*], Dinh Lam Bui [2,3]

[1] Faculty of Applied Sciences, Ton Duc Thang University, Ho Chi Minh City, Vietnam; phamminhtan@tdtu.edu.vn;
[2] Faculty of Biotechnology and Food Technology, Thai Nguyen University of Agriculture and Forestry, Thai Nguyen, Vietnam; buidinhlam@tuaf.edu.vn;
[3] Institute of Microbiology and Immunology, National Yang Ming Chiao Tung University, Taipei, Taiwan
* Correspondence: phamminhtan@tdtu.edu.vn;

Received: 27.10.2025; Accepted: 17.12.2025; Published: 15.04.2026

Abstract: N-[2-(2-Butyrylamino-ethoxy)-ethyl]-butyramide (BA-NH-NH-BA), a derivative of butyrate in fermentation metabolites of skin bacteria, can suppress the calcium phosphate (CaP)-induced itching, interleukin-6 (IL-6) production in skin, and activation of phosphorylated Bruton's tyrosine kinase (p-BTK) in dorsal root ganglion (DRG). By using IL-6 knockout (KO) mice, we verified that IL-6 was essential for CaP-induced activation of p-BTK in DRG. Data from western blotting showed that both butyrate and BA-NH-NH-BA at 4 mM effectively attenuated CaP-induced activation of p-BTK. Flow cytometry analysis revealed that the topical application of BA-NH-NH-BA at lower doses (< 4 mM) on mouse skin was sufficient to induce the acetylation on lysine 9 of histone H3 (AcH3K9) in keratinocytes. By knocking down free fatty acid receptor 2 (Ffar2) in mouse skin, we demonstrated that, unlike butyrate, BA-NH-NH-BA down-regulated the CaP-induced activation of p-BTK via an Ffar2-independent pathway. Exploring the biological mechanism underlying AcH3K9 and/or Ffar2 may expedite the development of BA-NH-NH-BA as a therapeutic for the treatment of uremic pruritus in patients with chronic kidney disease (CKD).

Keywords: butyric acid derivative; calcium phosphate; histone acetylation; interleukin-6; phosphorylated Bruton's tyrosine kinase.

1. Introduction

Chronic kidney disease (CKD) is a progressive loss of renal function affecting nearly 14% of adults in the United States and remains a major contributor to morbidity and mortality [1]. Pruritus is a frequent and burdensome symptom in CKD and has been linked to calcium phosphate (CaP) deposition in the skin, contributing to inflammation and impaired quality of life in dialysis patients [2-7]. Xerosis and chronic itch are particularly common among individuals undergoing hemodialysis or peritoneal dialysis [8-13]. Both central and peripheral mechanisms contribute to CKD-associated pruritus. Central sensitization involves G protein–coupled receptors (GPCRs) and downstream activation of extracellular signal–regulated kinase (ERK), which enhances spinal neuron excitability to pruritogens [14-16]. Peripherally, chronic elevation of interleukin-6 (IL-6) in serum and skin has been associated with inflammation and

adverse outcomes in CKD, suggesting that IL-6 plays a key role in itch-related signaling. Bruton's tyrosine kinase (BTK), a non-receptor kinase involved in immune cell activation, has also been implicated in renal inflammation, and BTK inhibition reduces disease severity in nephritis models [17,18].

Histone deacetylases (HDAC) inhibition has been shown to improve inflammatory and fibrotic markers in kidney disease models, supporting its potential as a therapeutic approach [19-21]. The inhibition of HDAC led to a dose-dependent reduction of IL-6 by inducing phosphorylation of signal transducer transcription 3 (STAT3) in naïve $CD4^+$ T-cells [22]. However, the molecular links between HDAC activity and IL-6 regulation are poorly understood.

Research has evidenced that short-chain fatty acids (SCFAs) are vital players in regulating inflammation through free fatty acid receptor 2 (Ffar2). Ffar2 is expressed in monocytes, neutrophils [23,24], regulatory T cells [25], and dendritic cells [26]. SCFAs like propionate and acetate can activate Ffar2 [27,28] through coupling to inositol 1,4,5-triphosphate formation, activation of extracellular signal-regulated kinase 1/2 (ERK 1/2), by intracellular Ca^{2+} release, and inhibition of cyclic adenosine monophosphate (cAMP) accumulation [28,29]. However, butyrate exerted its functions through either Ffar2 binding or HDAC inhibition [30,31]. Although SCFAs exhibit anti-inflammatory properties, their therapeutic use is limited by short half-lives and unfavorable physicochemical characteristics [32,33].

To address these limitations, we investigated BA-NH-NH-BA, a butyrate derivative with improved stability and solubility. This study examines whether BA-NH-NH-BA modulates CaP-induced IL-6, ERK, and phosphorylated BTK (p-BTK) signaling in keratinocytes and dorsal root ganglion (DRG), and whether its activity involves histone acetylation and Ffar2-associated pathways.

2. Materials and Methods

2.1. Administration of CaP and GLPG0974.

KERTr (keratinocytes transformed HPV 16 E6/E7 oncogenes) cells were added with 0, 0.05, 0.5, and 5 mg/mL of CaP. CaP (5 mg/ml) was injected subcutaneously into ICR mice to mimic the CKD-associated pruritic [34]. For Ffar2 inhibition, GLPG0974 (Ffar2 inhibitor) (Tocris Bioscience, Ellisville, MO, USA) was dissolved in dimethylsulfoxide (DMSO) (Sigma, St. Louis, MO, USA) to make a stock solution. Ffar2 was inhibited by gavage feeding of GLPG0974 (0.1–1 mg/kg) diluted in Phosphate buffer saline (PBS) (Gibco, Gaithersburg, MD, USA) [35], 20 min prior to topical application of butyrate or BA-NH-NH-BA, which was synthesized using a published protocol [36]. DMSO (0.1% in saline) was used as a vehicle control [37].

2.2. Western blotting.

A subcutaneous injection of calcium phosphate (CaP; 5 mg/mL) was delivered to the dorsal skin of ICR, WT, and IL-6-KO mice, followed 10 min later by topical treatment with at 4 mM, either as butyrate or BA-NH-NH-BA. A. In a separate experiment, the Ffar2 gene was silenced for 24 h by subcutaneous injection with scrambled or Ffar2 siRNA or gavage feeding with Ffar2 antagonist GLPG0974, followed by CaP (5 mg/mL) injection and application with 4 mM butyrate or BA-NH-NH-BA for 3 days. Dorsal root ganglion (DRG) was isolated after

2 h of CaP injection from ICR, IL-6 KO, and WT mice on the third day. In an in vitro experiment, KERTr cells were treated with or without 4 mM butyrate or BA-NH-NH-BA. The cell lysates or DRG homogenates ran through the 10% sodium dodecyl sulfate-polyacrylamide gel electrophoresis (SDS-PAGE), transferred to the polyvinylidene fluoride (PVDF) membrane (MilliporeSigma, Burlington, MA, USA) and subsequently blocked by the 5% (w/v) of bovine serum albumin (BSA) (Apolo Biochemical Inc., Hsinchu, Taiwan) for anti-BTK (phosphor Y550) (ab52192, 1:2,000) (Abcam, Cambridge, MA, USA) and 5% (w/v) of non-fat milk for β-actin (1:1,000, #4967, Cell Signaling, Danvers, MA, USA) before incubation overnight with respective antibodies. Next, followed by the secondary antibody, goat anti-rabbit (#G-21234) or anti-mouse (#G-21040) (1:5000; Thermo Fisher Scientific, Waltham, MA, USA), incubation for 1 h, chemiluminescent detection reagent, and Omega Lum^{TM} C Imaging System (Gel Company, San Francisco, CA, USA) was used for the detection of protein bands. Image J software was adopted for the densitometric analysis of protein bands.

2.3. Flow cytometry.

The C57BL/6 mice were used for flow cytometry analysis. The dorsal skin of mice was topically tested with 100 µL of PBS and 0.1, 0.4, 1, and 4 mM BA-NH-NH-BA in PBS for 2 h. The single-cell suspensions were prepared from mouse skin treated with BA-NH-NH-BA. Next, enzymatic digestion was pursued for 1 h with 2.5 mg/mL collagenase Type II and Type IV (Life Technologies, Grand Island, CA, USA) and 0.5 mg/mL DNase (Roche, IN, USA) in PBS containing 1% BSA at 37°C. Dulbecco's modified Eagle medium (DMEM) (Thermo Fisher Scientific) with 10% fetal bovine serum (FBS) was used for the quenching of digests. Subsequently, it was filtered with a 70 µM nylon filter (BD Bioscience, San Jose, CA, USA). DMEM containing 10% FBS was used for washing, followed by PBS/BSA. 0.01% formaldehyde (Polyscience, Warrington, PA, USA) was used for cell fixation, and 0.3% Triton was used for permeabilization (MilliporeSigma) before incubation with Alexa Fluor® 647 anti-acetylated lysine (Biolegend, San Diego, CA, USA) or Alexa Fluor® 448 anti-keratin 10 (K10) antibody [EP1607IHCY] (Abcam) at a dilution of 0.1 µg/mL in PBS/BSA for 1 h at 4°C. Guava EasyCyte 8HT two lasers were used for the analysis of cells, and a six-color microcapillary-based benchtop flow cytometer (MilliporeSigma) for assessing acetylation on lysine 9 of histone H3 (AcH3K9) and K10 expression. The stains of AcH3K9 and K10 were represented on the X-axis and Y-axis of the flow cytometry profile, respectively.

2.4. Ffar2 knockdown by siRNA.

The chemically modified Ffar2 siRNA was purchased from GenePharma Co. (Shanghai, China). A scramble siRNA, which did not target any known sequence, served as a negative control. The oligonucleotide sequences of siRNA for Ffar2 were the sense strand, 5'-CCGGUGCAGUACAAGUUAUTT-3' and anti-sense strand, 5'-AUAACUUGUACUGCACCGGTT-3'. The oligonucleotide sequences of scrambled siRNA were sense strand, 5'UUCUCCGAACGUGUCACGUTT and anti-sense strand, 5'-ACGUGACACGUUCGGAGAATT-3'. These chemically modified siRNAs (5 µM) were intradermally injected in the dorsal skin of ICR mice using microneedles to knock down the gene expression of Ffar2 [38,39].

2.5. Enzyme-linked immunosorbent assay (ELISA).

KERTr cells were treated with 0, 0.05, 0.5, and 5 mg/mL CaP, followed by lysis with a radioimmunoprecipitation assay (RIPA) buffer supplemented with ethylenediaminetetraacetic acid (EDTA)-free protease inhibitor cocktail (MilliporeSigma). Mouse skin samples were collected after 2 h of CaP injection. Cell or tissue lysates were extracted using tissue protein extraction reagent (T-PER^{TM}), and IL-6 was measured by a mouse (Catalog #DY406) or human (Catalog #DY206) ELISA assay kit (R&D Systems, Minneapolis, MN, USA) according to the manufacturer's protocol.

2.6. Statistical analysis.

Data analyses were performed by an unpaired *t*-test using GraphPad Prism software. The *p*-values of <0.05 (*), <0.01 (**), and <0.001 (***) were considered significant. At least three independent experiments were conducted to obtain the mean ± standard deviation (SD).

3. Results and Discussion

3.1. The essential role of IL-6 in CaP-induced p-BTK in DRG.

Disturbance in CaP metabolism with pruritus is a major problem associated with chronic dialysis patients with CKD. The human KERTr cells were treated with CaP (0-5 mg/ml) to mimic the CaP deposition in CKD patients. CaP-induced IL-6 secretion was detected by ELISA. As shown in Figure 1A, CaP induced IL-6 secretion from KERTr cells in a dose-dependent manner. The highest dose of 5 mg/mL CaP triggered the secretion of IL-6 at approximately 135 pg/mL. The IL-6 KO mice were used to investigate further the essential role of IL-6 in the CaP-induced signaling of p-BTK. The activation of p-BTK in DRG by CaP was dramatically suppressed when CaP was injected into the dorsal skin of IL-6 KO mice (Figure 1B), indicating that secretion of IL-6 from keratinocytes was essential for activation of p-BTK in DRG.

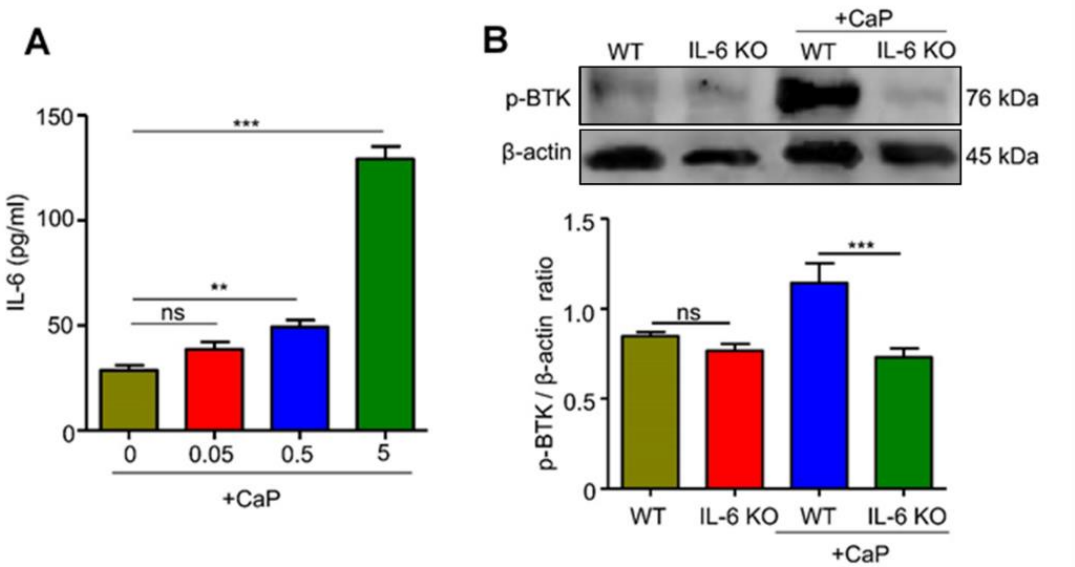

Figure 1. IL-6 regulated CaP-induced p-BTK expression. **(A)** Protein levels of IL-6 in KERTr cells treated with 0, 0.05, 0.5, and 5 mg/ml CaP were measured by ELISA; **(B)** Western blot analysis of p-BTK and β-actin in DRG of WT and IL-6 KO mice injected with/without CaP. The bar chart showed the ratio of intensities of p-BTK relative to β-actin. The mean ± SD was calculated from three independent experiments with 3 mice per group. The *p*-values of <0.01 (**) and <0.001 (***), were shown; ns = non-significant.

3.2. Inhibition of CaP-induced p-BTK by butyrate and BA-NH-NH-BA.

Results in our previous studies have shown that subcutaneous injection of CaP into mouse skin provoked scratching, increased the levels of IL-6 in skin, and p-ERK 1/2 in DRG. The CaP-induced scratching and an increase in IL-6 and p-ERK 1/2 were significantly ameliorated by the topical application of 4 mM butyrate or BA-NH-NH-BA onto CaP-injected skin. Although p-BTK in DRG can be detectable after subcutaneous injection of CaP [40], it is not clear whether the topical application of butyrate or BA-NH-NH-BA affects the CaP-induced activation of p-BTK. As shown in Figure 2, a significant reduction in p-BTK in DRG was detected after the topical application of butyrate or BA-NH-NH-BA onto the CaP-injected skin (Figure 2), demonstrating the inhibitory effects of both butyrate and BA-NH-NH-BA on CaP-induced activation of p-BTK in DRG.

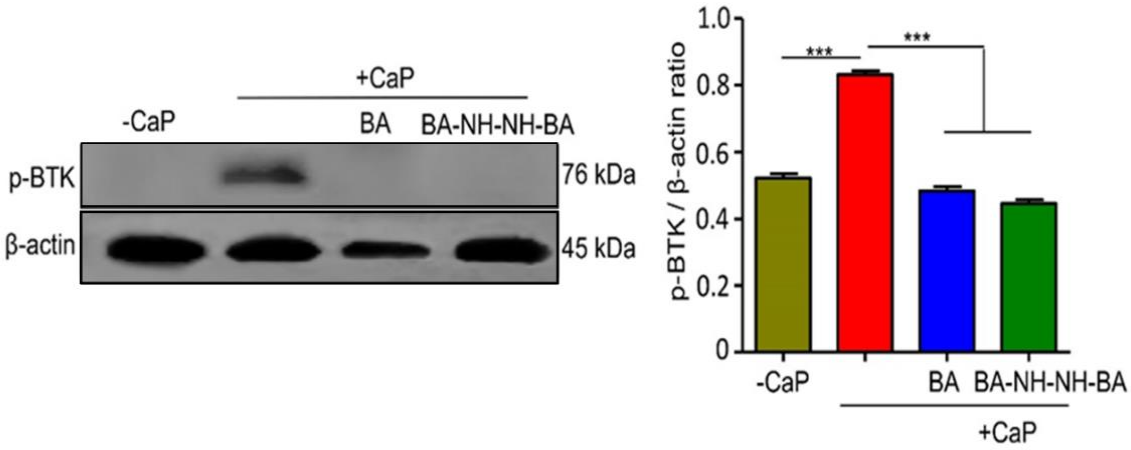

Figure 2. Inhibition of CaP-induced p-BTK expression in DRG of mice by 4 mM butyrate (BA) or BA-NH-NH-BA. Western blot analyses of p-BTK and β-actin in DRG of CaP-injected mice, and topically applied with BA or BA-NH-NH-BA, were performed. The ratios of intensities of p-BTK relative to β-actin were shown. The mean ± SD was calculated for three independent experiments. Three mice per group were used. The *p*-value <0.001 (***)was indicated.

3.3. Dose-dependent induction of AcH3K9 by BA-NH-NH-BA.

It has been reported that 4 mM, but not a lower dose, of butyrate can inhibit the HDAC [41]. Mouse skin wounds, pretreated with butyrate or BA-NH-NH-BA, can effectively induce the AcH3K9 in keratinocytes [42]. To determine the efficacy of low doses of BA-NH-NH-BA to induce AcH3K9 in vivo, the dorsal skin of C57BL/6 mice was topically applied with 0.1, 0.4, 1, and 4 mM BA-NH-NH-BA for 2 h. The induction of AcH3K9 in keratinocytes was gated for K10 in flow cytometry analysis. As shown in Figure 3, more than fifty-five percent of single cells of mouse skin were identified as AcH3K9 and K10 double positive. A significant increase in the percentage of AcH3K9 and K10 double-positive cells was observed when mouse skin was topically applied with 0.1 mM BA-NH-NH-BA. The higher percentages of AcH3K9 and K10 double-positive cells were detected with an increase in dose (0.4, 1, or 4 mM) of BA-NH-NH-BA (Figure 3). The result demonstrated the histone acetylation property of BA-NH-NH-BA at lower doses.

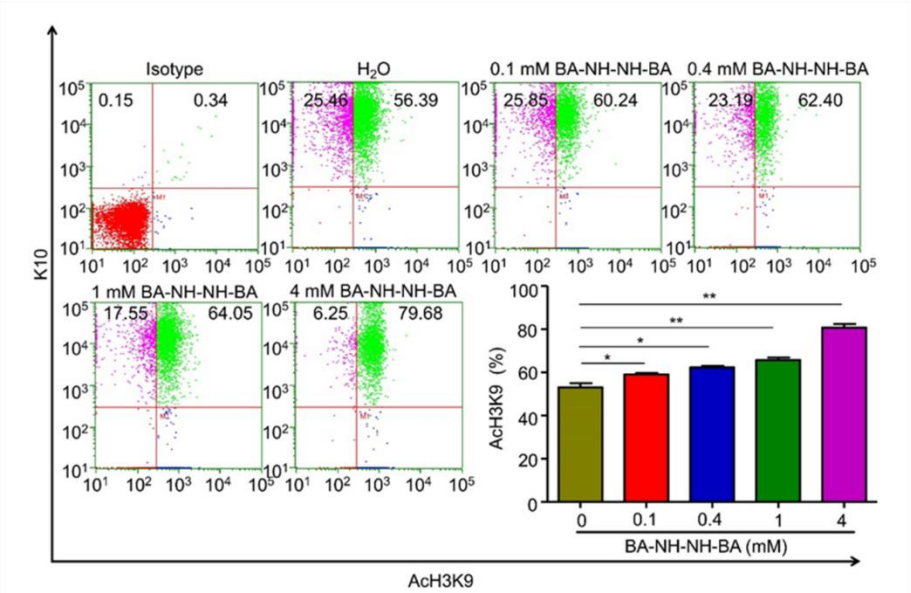

Figure 3. Induction of AcH3K9 by different doses of BA-NH-NH-BA. Flow cytometry was conducted to detect AcH3K9 in the single-cell suspension of mouse skin treated with H_2O or 0.1, 0.4, 1, and 4 mM BA-NH-NH-BA. Antibodies to K10, a marker for differentiated keratinocytes, and AcH3K9 were used for staining. Isotype was used as a control to identify the non-specific background staining. The bar graph represented the percentage (%) of cells positively stained with both AcH3K9 and K10. The *p*-values of <0.05 (*), <0.01 (**), and <0.001 (***) from three different experiments with mean ± SD were shown.

3.4. No effect of Ffar2 knockdown on the attenuation of CaP-induced p-BTK by BA-NH-NH-BA.

Anti-inflammatory activity of butyrate can be triggered by the binding of butyrate to Ffar2 [43,44]. Inhibition of HDACs is also a molecular mode of action of butyrate or propionate, but not acetate, to reduce inflammation [42,45]. Interestingly, overexpression of HDACs was observed in a Ffar2-deficient mouse model of colorectal cancer, leading to the development of colon adenomas and the further progression to adenocarcinoma, revealing a crucial role of epigenetic changes in the process of disease progression [46,47]. To determine if inhibition of CaP-induced p-BTK by butyrate or BA-NH-NH-BA is mediated by Ffar2, an *in vivo* approach for knockdown of the Ffar2 expression in mouse skin by subcutaneous injection of Ffar2 siRNA and by gavage feeding of Ffar2 selective antagonist GLPG0974 (0.1–1 mg/kg). Results from western blotting in Figure 4A, 4B showed that the knockdown of Ffar2 by its specific siRNA or GLPG0974 as a specific antagonist significantly blocked the inhibitory action of butyrate, but not BA-NH-NH-BA, on CaP-induced activation of p-BTK. The result demonstrated that, unlike butyrate, BA-NH-NH-BA inhibited the CaP-induced activation of p-BTK, which was independent of Ffar2. On combining results here and from other publications [40,48], subcutaneous injection of CaP into mouse skin induced secretion of IL-6 from keratinocytes. IL-6 is essential for CaP to induce the activation of p-BTK in DRG (Figure 1). Butyrate may exhibit dual action, concurrently inducing AcH3K9 and binding to Ffar2, thereby diminishing CaP-induced activation of p-BTK in DRG. However, BA-NH-NH-BA, as an epigenetic drug, induced AcH3K9 in keratinocytes independent of Ffar2 to down-regulate the CaP-induced activation of p-BTK in DRG (Figure 4C).

The present study demonstrates that CaP-induced activation of p-BTK in the DRG requires IL-6 derived from keratinocytes. This is supported by the absence of p-BTK induction in IL-6 KO mice and is consistent with previous reports linking CaP exposure to increased IL-6 expression and activation of downstream signaling pathways, including p-ERK and p-BTK,

in models of uremic pruritus [49-52]. The enhancement of p-BTK expression by recombinant IL-6 further reinforces the role of IL-6 as an upstream regulator in this pathway, although the feedback effect of BTK inhibition on IL-6 levels noted in earlier studies warrants additional investigation [53,54].

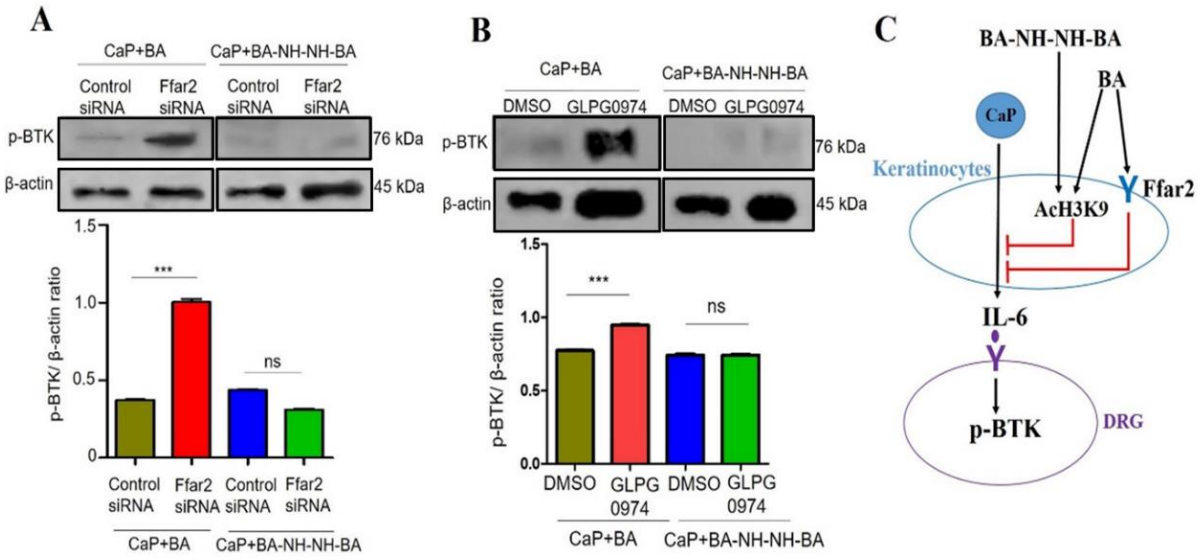

Figure 4. Regulation of CaP-induced p-BTK expression by butyrate (BA) or BA-NH-NH-BA in response to Ffar2 and HDAC *in vivo*. Western blot analyses of p-BTK and β-actin in DRG of CaP-induced mice subcutaneously injected with scrambled or Ffar2 siRNA (**A)** or gavage feeding with GLPG0974 or DMSO; **(B)** 10 min prior to topical application with BA or BA-NH-NH-BA. The ratios of intensities of p-BTK relative to β-actin from both experiments are shown. The mean ± SD was calculated for three separate experiments using three mice per group with *p*-values <0.001 (***); ns = non-significant; **(C)** The signaling pathway of CaP-induced secretion of IL-6 from KERTr cells, activation of p-BTK in DRG, and further targeting this signaling by BA or BA-NH-NH-BA treatment through Ffar2 or AcH3K9 mediated mechanism is proposed.

Topical butyrate and BA-NH-NH-BA attenuated CaP-induced p-BTK activation. These findings align with prior evidence showing that HDAC inhibition can reduce inflammatory signaling, including BTK activation, in immune-related disorders [42,55,56]. Compared with butyrate, BA-NH-NH-BA induced AcH3K9 at substantially lower doses, consistent with the enhanced epigenetic activity reported for certain butyrate derivatives and co-drugs [57-62]. The favorable solubility and stability profile of BA-NH-NH-BA may further support its potential as a therapeutic candidate relative to naturally occurring SCFAs [36].

Our data also reveal mechanistic differences between butyrate and BA-NH-NH-BA in relation to Ffar2. While Ffar2 knockdown or antagonism compromised the inhibitory effect of butyrate on p-BTK, BA-NH-NH-BA remained effective under the same conditions. This distinction is consistent with previous findings showing that SCFAs can act through both receptor-dependent and HDAC-dependent mechanisms, and that HDAC inhibition can occur independently of Ffar2 signaling [63-65]. The reduced affinity of BA-NH-NH-BA for Ffar2 due to its extended carbon structure provides a plausible explanation for this independence [66].

Overall, our findings suggest that BA-NH-NH-BA suppresses CaP-induced pruritic signaling primarily through epigenetic regulation, including the induction of AcH3K9 and modulation of IL-6–dependent pathways affecting p-BTK. While this study supports a mechanistic framework involving HDAC-associated signaling, additional work will be needed to delineate further the molecular interactions linking BA-NH-NH-BA, histone acetylation, IL-6 regulation, and neuronal activation in the DRG [67-70].

4. Conclusions

The findings of this study indicate that BA-NH-NH-BA and butyrate can attenuate CaP-induced p-BTK activation, with IL-6 serving as an upstream regulator in this pathway, and that BA-NH-NH-BA is able to induce AcH3K9 at lower doses. While these results suggest potential epigenetic and receptor-independent effects of BA-NH-NH-BA, the current data are not sufficient to establish definitive mechanistic pathways. Therefore, the proposed actions involving Ffar2 independence and histone acetylation should be interpreted cautiously, and further studies will be required to validate these mechanistic hypotheses and clarify their relevance to uremic pruritus. It has been shown that topical application of fermenting *Cutibacterium acnes* (*C. acnes*), butyrate, and its derivative BA-NH-NH-BA significantly suppressed the CaP-induced IL-6 in skin [71,72], illustrating the potential to develop fermentation metabolites as postbiotics for treatment of uremic pruritus [73,74].

Author Contributions

Conceptualization, D.L.B.; methodology, M.T.P.; formal analysis, M.T.P.; investigation, M.T.P.; writing—original draft preparation, M.T.P.; writing—review and editing, D.L.B.; supervision, D.L.B. All authors have read and agreed to the published version of the manuscript. D.L.B. is the guarantor of this work.

Institutional Review Board Statement

The animal study protocol was approved by the local animal use committee (IACUC 1100508, National Yang-Ming Chiao-Tung University, Taiwan). All animal care followed the Guide for the Use of Laboratory Animals (US National Research Council). Institute of Cancer Research (ICR), IL-6 knockout (KO), and wild type (WT) C57BL/6 mice (8 to 9-week-old female; National Laboratory Animal Center, Taipei, Taiwan) were used for scarification by the asphyxiation method with CO_2. The outbred strain of ICR mice was used as they express genetic variability similar to that naturally occurring in human populations [75]. The C57BL/6 strain could be manipulated genetically for the study of cytokine expressions, such as IL-6 and the inflammatory acute-phase response after tissue damage or infection [76].

Informed Consent Statement

Not applicable.

Data Availability Statement

Data supporting the findings of this study are available upon reasonable request from the corresponding author.

Funding

This research received no external funding.

Acknowledgments

This work was supported by Ton Duc Thang University.

Conflicts of Interest

The authors declare no conflict of interest.

References

1. Collins, A.J.; Foley, R.N.; Gilbertson, D.T.; Chen, S.-C. United States Renal Data System public health surveillance of chronic kidney disease and end-stage renal disease. *Kidney Int. Suppl.* **2015**, *5*, 2-7, https://doi.org/10.1038/kisup.2015.2.
2. Locatelli, F.; Pozzoni, P.; Tentori, F.; Del Vecchio, L. Epidemiology of cardiovascular risk in patients with chronic kidney disease. *Nephrol. Dial. Transplant.* **2003**, *18*, vii2-vii9, https://doi.org/10.1093/ndt/gfg1072.
3. Moe, S.; Drüeke, T.; Cunningham, J.; Goodman, W.; Martin, K.; Olgaard, K.; Ott, S.; Sprague, S.; Lameire, N.; Eknoyan, G. Definition, evaluation, and classification of renal osteodystrophy: A position statement from Kidney Disease: Improving Global Outcomes (KDIGO). *Kidney Int.* **2006**, *69*, 1945-1953, https://doi.org/10.1038/sj.ki.5000414.
4. Vaziri, N.D. Dyslipidemia of chronic renal failure: the nature, mechanisms, and potential consequences. *Am. J. Physiol. Renal Physiol.* **2006**, *290*, F262-F272, https://doi.org/10.1152/ajprenal.00099.2005.
5. Brancaccio, D.; Tetta, C.; Gallieni, M.; Panichi, V. Inflammation, CRP, calcium overload and a high calcium–phosphate product: a *'liaison dangereuse'*. *Nephrol. Dial. Transplant.* **2002**, *17*, 201-203, https://doi.org/10.1093/ndt/17.2.201.
6. Pisoni, R.L.; Wikström, B.; Elder, S.J.; Akizawa, T.; Asano, Y.; Keen, M.L.; Saran, R.; Mendelssohn, D.C.; Young, E.W.; Port, F.K. Pruritus in haemodialysis patients: International results from the Dialysis Outcomes and Practice Patterns Study (DOPPS). *Nephrol. Dial. Transplant.* **2006**, *21*, 3495-3505, https://doi.org/10.1093/ndt/gfl461.
7. Lavery, M.J.; Stull, C.; Kinney, M.O.; Yosipovitch, G. Nocturnal Pruritus: The Battle for a Peaceful Night's Sleep. *Int. J. Mol. Sci.* **2016**, *17*, 425, https://doi.org/10.3390/ijms17030425.
8. Heisig, M.; Reich, A.; Szepietowski, J.C. Is uremic pruritus still an important clinical problem in maintenance hemodialysis patients? *J. Eur. Acad. Dermatol. Venereol.* **2016**, *30*, e198-e199, https://doi.org/10.1111/jdv.13524.
9. Solak, B.; Acikgoz, S.B.; Sipahi, S.; Erdem, T. Epidemiology and determinants of pruritus in pre-dialysis chronic kidney disease patients. *Int. Urol. Nephrol.* **2016**, *48*, 585-591, https://doi.org/10.1007/s11255-015-1208-5.
10. Shirazian, S.; Aina, O.; Park, Y.; Chowdhury, N.; Leger, K.; Hou, L.; Miyawaki, N.; Mathur, V.S. Chronic kidney disease-associated pruritus: impact on quality of life and current management challenges. *Int. J. Nephrol. Renovasc. Dis.* **2017**, *10*, 11-26, https://doi.org/10.2147/ijnrd.s108045.
11. Suseł, J.; Batycka-Baran, A.; Reich, A.; Szepietowski, J.C. Uraemic Pruritus Markedly Affects the Quality of Life and Depressive Symptoms in Haemodialysis Patients with End-stage Renal Disease. *Acta Derm.-Venereol.* **2013**, *94*, 276-281, https://doi.org/10.2340/00015555-1749.
12. Weiss, M.; Mettang, T.; Tschulena, U.; Passlick-Deetjen, J.; Weisshaar, E. Prevalence of Chronic Itch and Associated Factors in Haemodialysis Patients: A Representative Cross-sectional Study. *Acta Derm.-Venereol.* **2015**, *95*, 816-821, https://doi.org/10.2340/00015555-2087.
13. Morton, C.A.; Lafferty, M.; Hau, C.; Henderson, I.; Jones, M.; Lowe, J.G. Pruritus and skin hydration during dialysis. *Nephrol. Dial. Transplant.* **1996**, *11*, 2031-2036, https://doi.org/10.1093/oxfordjournals.ndt.a027092.
14. Bautista, D.M.; Wilson, S.R.; Hoon, M.A. Why we scratch an itch: the molecules, cells and circuits of itch. *Nat. Neurosci.* **2014**, *17*, 175-182, https://doi.org/10.1038/nn.3619.
15. Liu, T.; Ji, R.-R. New insights into the mechanisms of itch: are pain and itch controlled by distinct mechanisms?. *Pflugers Arch. Eur. J. Physiol.* **2013**, *465*, 1671-1685, https://doi.org/10.1007/s00424-013-1284-2.
16. Zhang, L.; Jiang, G.-Y.; Song, N.-J.; Huang, Y.; Chen, J.-Y.; Wang, Q.-X.; Ding, Y.-Q. Extracellular signal-regulated kinase (ERK) activation is required for itch sensation in the spinal cord. *Mol. Brain* **2014**, *7*, 25, https://doi.org/10.1186/1756-6606-7-25.
17. Chalmers, S.A.; Doerner, J.; Bosanac, T.; Khalil, S.; Smith, D.; Harcken, C.; Dimock, J.; Der, E.; Herlitz, L.; Webb, D.; Seccareccia, E.; Feng, D.; Fine, J.S.; Ramanujam, M.; Klein, E.; Putterman, C. Therapeutic

Blockade of Immune Complex-Mediated Glomerulonephritis by Highly Selective Inhibition of Bruton's Tyrosine Kinase. *Sci. Rep.* **2016**, *6*, 26164, https://doi.org/10.1038/srep26164.
18. Kong, W.; Deng, W.; Sun, Y.; Huang, S.; Zhang, Z.; Shi, B.; Chen, W.; Tang, X.; Yao, G.; Feng, X.; Sun, L. Increased expression of Bruton's tyrosine kinase in peripheral blood is associated with lupus nephritis. *Clin. Rheumatol.* **2018**, *37*, 43-49, https://doi.org/10.1007/s10067-017-3717-3.
19. Lisiero, D.N.; Soto, H.; Everson, R.G.; Liau, L.M.; Prins, R.M. The histone deacetylase inhibitor, LBH589, promotes the systemic cytokine and effector responses of adoptively transferred CD8+ T cells. *J. Immunother. Cancer* **2014**, *2*, 8, https://doi.org/10.1186/2051-1426-2-8.
20. Liu, N.; Zhuang, S. Treatment of chronic kidney diseases with histone deacetylase inhibitors. *Front. Physiol.* **2015**, *6*, 121, https://doi.org/10.3389/fphys.2015.00121.
21. Regna, N.L.; Chafin, C.B.; Hammond, S.E.; Puthiyaveetil, A.G.; Caudell, D.L.; Reilly, C.M. Class I and II histone deacetylase inhibition by ITF2357 reduces SLE pathogenesis in vivo. *Clin. Immunol.* **2014**, *151*, 29-42, https://doi.org/10.1016/j.clim.2014.01.002.
22. Yang, X.O.; Panopoulos, A.D.; Nurieva, R.; Chang, S.H.; Wang, D.; Watowich, S.S.; Dong, C. STAT3 Regulates Cytokine-mediated Generation of Inflammatory Helper T Cells*. *J. Biol. Chem.* **2007**, *282*, 9358-9363, https://doi.org/10.1074/jbc.C600321200.
23. Sivaprakasam, S.; Prasad, P.D.; Singh, N. Benefits of short-chain fatty acids and their receptors in inflammation and carcinogenesis. *Pharmacol. Ther.* **2016**, *164*, 144-151, https://doi.org/10.1016/j.pharmthera.2016.04.007.
24. Sawzdargo, M.; George, S.R.; Nguyen, T.; Xu, S.; Kolakowski, L.F.; O'Dowd, B.F. A Cluster of Four Novel Human G Protein-Coupled Receptor Genes Occurring in Close Proximity to CD22 Gene on Chromosome 19q13.1. *Biochem. Biophys. Res. Commun.* **1997**, *239*, 543-547, doi:https://doi.org/10.1006/bbrc.1997.7513.
25. Nakao, S.; Fujii, A.; Niederman, R. Alteration of cytoplasmic Ca2+ in resting and stimulated human neutrophils by short-chain carboxylic acids at neutral pH. *Infect. Immun.* **1992**, *60*, 5307-5311, https://doi.org/10.1128/iai.60.12.5307-5311.1992.
26. Nakao, S.; Moriya, Y.; Furuyama, S.; Niederman, R.; Sugiya, H. PROPIONIC ACID STIMULATES SUPEROXIDE GENERATION IN HUMAN NEUTROPHILS. *Cell Biol. Int.* **1998**, *22*, 331-337, https://doi.org/10.1006/cbir.1998.0263.
27. Smith, P.M.; Howitt, M.R.; Panikov, N.; Michaud, M.; Gallini, C.A.; Bohlooly-Y, M.; Glickman, J.N.; Garrett, W.S. The Microbial Metabolites, Short-Chain Fatty Acids, Regulate Colonic T_{reg} Cell Homeostasis. *Science* **2013**, *341*, 569-573, https://doi.org/10.1126/science.1241165.
28. Trompette, A.; Gollwitzer, E.S.; Yadava, K.; Sichelstiel, A.K.; Sprenger, N.; Ngom-Bru, C.; Blanchard, C.; Junt, T.; Nicod, L.P.; Harris, N.L.; Marsland, B.J. Gut microbiota metabolism of dietary fiber influences allergic airway disease and hematopoiesis. *Nat. Med.* **2014**, *20*, 159-166, https://doi.org/10.1038/nm.3444.
29. Brown, A.J.; Jupe, S.; Briscoe, C.P. A Family of Fatty Acid Binding Receptors. *DNA Cell Biol.* **2005**, *24*, 54-61, https://doi.org/10.1089/dna.2005.24.54.
30. Nilsson, N.E.; Kotarsky, K.; Owman, C.; Olde, B. Identification of a free fatty acid receptor, FFA_2R, expressed on leukocytes and activated by short-chain fatty acids. *Biochem. Biophys. Res. Commun.* **2003**, *303*, 1047-1052, https://doi.org/10.1016/S0006-291X(03)00488-1.
31. Le Poul, E.; Loison, C.; Struyf, S.; Springael, J.-Y.; Lannoy, V.; Decobecq, M.-E.; Brezillon, S.; Dupriez, V.; Vassart, G.; Van Damme, J.; Parmentier, M.; Detheux, M. Functional Characterization of Human Receptors for Short Chain Fatty Acids and Their Role in Polymorphonuclear Cell Activation*. *Biol. Chem.* **2003**, *278*, 25481-25489, https://doi.org/10.1074/jbc.M301403200.
32. Liu, H.; Wang, J.; He, T.; Becker, S.; Zhang, G.; Li, D.; Ma, X. Butyrate: A Double-Edged Sword for Health?. *Adv. Nutr.* **2018**, *9*, 21-29, https://doi.org/10.1093/advances/nmx009.
33. Tan, J.; McKenzie, C.; Potamitis, M.; Thorburn, A.N.; Mackay, C.R.; Macia, L. Chapter Three - The Role of Short-Chain Fatty Acids in Health and Disease. In Advances in Immunology; Alt, F.W., Ed.; Academic Press: **2014**; Volume 121, pp. 91-119, https://doi.org/10.1016/B978-0-12-800100-4.00003-9.
34. Jeong, Y.; Du, R.; Zhu, X.; Yin, S.; Wang, J.; Cui, H.; Cao, W.; Lowenstein, C.J. Histone deacetylase isoforms regulate innate immune responses by deacetylating mitogen-activated protein kinase phosphatase-1. *J. Leukocyte Biol.* **2014**, *95*, 651-659, https://doi.org/10.1189/jlb.1013565.
35. Huang, W.; Zhou, L.; Guo, H.; Xu, Y.; Xu, Y. The role of short-chain fatty acids in kidney injury induced by gut-derived inflammatory response. *Metabolism* **2017**, *68*, 20-30, https://doi.org/10.1016/j.metabol.2016.11.006.

36. Roy, D.K. Pruritus in chronic kidney disease: A frustrating symptom. *Bangladesh Renal J.* **2007**, 26, 47-54.
37. raisaeng, S.; Batsukh, A.; Chuang, T.-H.; Herr, D.R.; Huang, Y.-F.; Chimeddorj, B.; Huang, C.-M. Leuconostoc mesenteroides fermentation produces butyric acid and mediates Ffar2 to regulate blood glucose and insulin in type 1 diabetic mice. *Sci. Rep.* **2020**, *10*, 7928, https://doi.org/10.1038/s41598-020-64916-2.
38. Traisaeng, S.; Herr, D.R.; Kao, H.-J.; Chuang, T.-H.; Huang, C.-M. A Derivative of Butyric Acid, the Fermentation Metabolite of *Staphylococcus epidermidis*, Inhibits the Growth of a *Staphylococcus aureus* Strain Isolated from Atopic Dermatitis Patients. *Toxins* **2019**, *11*, 311, https://doi.org/10.3390/toxins11060311.
39. Bao, Z.; Guan, S.; Cheng, C.; Wu, S.; Wong, S.H.; Kemeny, D.M.; Leung, B.P.; Wong, W.S.F. A novel antiinflammatory role for andrographolide in asthma via inhibition of the nuclear factor-κB pathway. *Am. J. Respir. Crit. Care Med.* **2009**, *179*, 657-665, https://doi.org/10.1164/rccm.200809-1516oc.
40. Pan, J.; Ruan, W.; Qin, M.; Long, Y.; Wan, T.; Yu, K.; Zhai, Y.; Wu, C.; Xu, Y. Intradermal delivery of STAT3 siRNA to treat melanoma via dissolving microneedles. *Sci. Rep.* **2018**, *8*, 1117, https://doi.org/10.1038/s41598-018-19463-2.
41. Pizzonero, M.; Dupont, S.; Babel, M.; Beaumont, S.; Bienvenu, N.; Blanqué, R.; Cherel, L.; Christophe, T.; Crescenzi, B.; De Lemos, E.; Delerive, P.; Deprez, P.; De Vos, S.; Djata, F.; Fletcher, S.; Kopiejewski, S.; L'Ebraly, C.; Lefrançois, J.-M.; Lavazais, S.; Manioc, M.; Nelles, L.; Oste, L.; Polancec, D.; Quénéhen, V.; Soulas, F.; Triballeau, N.; van der Aar, E.M.; Vandeghinste, N.; Wakselman, E.; Brys, R.; Saniere, L. Discovery and Optimization of an Azetidine Chemical Series As a Free Fatty Acid Receptor 2 (FFA2) Antagonist: From Hit to Clinic. *J. Med. Chem.***2014**, *57*, 10044-10057, https://doi.org/10.1021/jm5012885.
42. Zhou, Q.; Wu, C.; Zha, J.; Ge, J.; Yan, Q.; Wang, Y.; Song, D.; Zou, J. Calcium Phosphate Cement Causes Nucleus Pulposus Cell Degeneration Through the ERK Signaling Pathway. *Open Life Sci.* **2020**, *15*, 209-216, https://doi.org/10.1515/biol-2020-0021.
43. Hamlet, S.; Ivanovski, S. Inflammatory cytokine response to titanium chemical composition and nanoscale calcium phosphate surface modification. *Acta Biomater.* **2011**, *7*, 2345-2353, https://doi.org/10.1016/j.actbio.2011.01.032.
44. Cohen, E.P.; Russell, T.J.; Garancis, J.C. Mast Cells and Calcium in Severe Uremic Itching. *The American J. Med. Sci.* **1992**, *303*, 360-365, https://doi.org/10.1097/00000441-199206000-00002.
45. McDonald, C.; Xanthopoulos, C.; Kostareli, E. The role of Bruton's tyrosine kinase in the immune system and disease. *Immunology* **2021**, *164*, 722-736, https://doi.org/10.1111/imm.13416.
46. Darlenski, R.; Kozyrskyj, A.L.; Fluhr, J.W.; Caraballo, L. Association between barrier impairment and skin microbiota in atopic dermatitis from a global perspective: Unmet needs and open questions. *J. Allergy Clin. Immunol.* **2021**, *148*, 1387-1393, https://doi.org/10.1016/j.jaci.2021.10.002.
47. D'Hooghe, T.M.; Vanhie, A.; Flores, V.A.; Taylor, H.S. Macrophage depletion: a potential immunomodulator treatment of endometriosis-associated pain? *Ann. Transl. Med.* **2020**, *8*, 1534, https://doi.org/10.21037/atm-2020-98.
48. Elhag, S.; Rivas, N.; Tejovath, S.; Mustaffa, N.; Deonarine, N.; Hashmi, M.A.; Yerneni, S.; Hamid, P.; Hashmi, M.A.; Hamid, P.F. Chronic kidney disease-associated pruritus: a glance at novel and lesser-known treatments. *Cureus* **2022**, *14*, e21127, https://doi.org/10.7759/cureus.21127.
49. Bassani, C.; Molinari, M.; Romeo, V.; Martinelli, V.; Boschert, U.; Martino, G.; Muzio, L.; Farina, C. The contribution of BTK signaling in myeloid cells to neuroinflammation. *Front. Immunol.* **2025**, *16*, 1595069, https://doi.org/10.3389/fimmu.2025.1595069.
50. Nam, H.Y.; Nam, J.H.; Yoon, G.; Lee, J.-Y.; Nam, Y.; Kang, H.-J.; Cho, H.-J.; Kim, J.; Hoe, H.-S. Ibrutinib suppresses LPS-induced neuroinflammatory responses in BV2 microglial cells and wild-type mice. *J. Neuroinflammat.* **2018**, *15*, 271, https://doi.org/10.1186/s12974-018-1308-0.
51. Ericsson, A.C.; Davis, D.J.; Franklin, C.L.; Hagan, C.E. Exoelectrogenic capacity of host microbiota predicts lymphocyte recruitment to the gut. *Physiol. Genomics* **2015**, *47*, 243-252, https://doi.org/10.1152/physiolgenomics.00010.2015.
52. Schmidt, A.D.; de Guzman Strong, C. Current understanding of epigenetics in atopic dermatitis. *Exp. Dermatol.* **2021**, *30*, 1150-1155, https://doi.org/10.1111/exd.14392.
53. Jain, P.; Keating, M.; Wierda, W.; Estrov, Z.; Ferrajoli, A.; Jain, N.; George, B.; James, D.; Kantarjian, H.; Burger, J.; O'Brien, S. Outcomes of patients with chronic lymphocytic leukemia after discontinuing ibrutinib. *Blood* **2015**, *125*, 2062-2067, https://doi.org/10.1182/blood-2014-09-603670.

54. Bottoni, A.; Rizzotto, L.; Lai, T.-H.; Liu, C.; Smith, L.L.; Mantel, R.; Reiff, S.; El-Gamal, D.; Larkin, K.; Johnson, A.J.; Lapalombella, R.; Lehman, A.; Plunkett, W.; Byrd, J.C.; Blachly, J.S.; Woyach, J.A.; Sampath, D. Targeting BTK through microRNA in chronic lymphocytic leukemia. *Blood* **2016**, *128*, 3101-3112, https://doi.org/10.1182/blood-2016-07-727750.
55. Donohoe, Dallas R.; Collins, Leonard B.; Wali, A.; Bigler, R.; Sun, W.; Bultman, Scott J. The Warburg Effect Dictates the Mechanism of Butyrate-Mediated Histone Acetylation and Cell Proliferation. *Mol. Cell* **2012**, *48*, 612-626, https://doi.org/10.1016/j.molcel.2012.08.033.
56. Kim, S.W.; Hooker, J.M.; Otto, N.; Win, K.; Muench, L.; Shea, C.; Carter, P.; King, P.; Reid, A.E.; Volkow, N.D.; Fowler, J.S. Whole-body pharmacokinetics of HDAC inhibitor drugs, butyric acid, valproic acid and 4-phenylbutyric acid measured with carbon-11 labeled analogs by PET. *Nucl. Med. Biol.* **2013**, *40*, 912-918, https://doi.org/10.1016/j.nucmedbio.2013.06.007.
57. Bianchi, N.; Chiarabelli, C.; Zuccato, C.; Lampronti, I.; Borgatti, M.; Amari, G.; Delcanale, M.; Chiavilli, F.; Prus, E.; Fibach, E.; Gambari, R. Erythroid differentiation ability of butyric acid analogues: Identification of basal chemical structures of new inducers of foetal haemoglobin. *Eur. J. Pharmacol.* **2015**, *752*, 84-91, https://doi.org/10.1016/j.ejphar.2015.02.018.
58. Wang, Y.; Zhang, L.; Yu, J.; Huang, S.; Wang, Z.; Chun, K.A.; Lee, T.L.; Chen, Y.-T.; Gallo, R.L.; Huang, C.-M. A Co-Drug of Butyric Acid Derived from Fermentation Metabolites of the Human Skin Microbiome Stimulates Adipogenic Differentiation of Adipose-Derived Stem Cells: Implications in Tissue Augmentation. *J. Investig. Dermatol.* **2017**, *137*, 46-56, https://doi.org/10.1016/j.jid.2016.07.030.
59. Shimazu, T.; Hirschey, M.D.; Newman, J.; He, W.; Shirakawa, K.; Le Moan, N.; Grueter, C.A.; Lim, H.; Saunders, L.R.; Stevens, R.D.; Newgard, C.B.; Farese, R.V.; de Cabo, R.; Ulrich, S.; Akassoglou, K.; Verdin, E. Suppression of Oxidative Stress by β-Hydroxybutyrate, an Endogenous Histone Deacetylase Inhibitor. *Science* **2013**, *339*, 211-214, https://doi.org/10.1126/science.1227166.
60. Hamer, H.M.; Jonkers, D.; Venema, K.; Vanhoutvin, S.; Troost, F.J.; Brummer, R.J. Review article: the role of butyrate on colonic function. *Aliment. Pharmacol. Ther.* **2008**, *27*, 104-119, https://doi.org/10.1111/j.1365-2036.2007.03562.x.
61. Zheng, L.; Kelly, C.J.; Battista, K.D.; Schaefer, R.; Lanis, J.M.; Alexeev, E.E.; Wang, R.X.; Onyiah, J.C.; Kominsky, D.J.; Colgan, S.P. Microbial-Derived Butyrate Promotes Epithelial Barrier Function through IL-10 Receptor–Dependent Repression of Claudin-2. *J. Immunol.* **2017**, *199*, 2976-2984, https://doi.org/10.4049/jimmunol.1700105.
62. Nadeem, A.; Ahmad, S.F.; Al-Harbi, N.O.; El-Sherbeeny, A.M.; Al-Harbi, M.M.; Almukhlafi, T.S. GPR43 activation enhances psoriasis-like inflammation through epidermal upregulation of IL-6 and dual oxidase 2 signaling in a murine model. *Cell. Signal.* **2017**, *33*, 59-68, https://doi.org/10.1016/j.cellsig.2017.02.014.
63. Pan, P.; Oshima, K.; Huang, Y.-W.; Agle, K.A.; Drobyski, W.R.; Chen, X.; Zhang, J.; Yearsley, M.M.; Yu, J.; Wang, L.-S. Loss of FFAR2 promotes colon cancer by epigenetic dysregulation of inflammation suppressors. *Int. J. Cancer* **2018**, *143*, 886-896, https://doi.org/10.1002/ijc.31366.
64. Park, J.; Kim, M.; Kang, S.G.; Jannasch, A.H.; Cooper, B.; Patterson, J.; Kim, C.H. Short-chain fatty acids induce both effector and regulatory T cells by suppression of histone deacetylases and regulation of the mTOR–S6K pathway. *Mucosal Immunol.* **2015**, *8*, 80-93, https://doi.org/10.1038/mi.2014.44.
65. Pirozzi, C.; Francisco, V.; Guida, Francesca D.; Gómez, R.; Lago, F.; Pino, J.; Meli, R.; Gualillo, O. Butyrate Modulates Inflammation in Chondrocytes via GPR43 Receptor. *Cell. Physiol. Biochem.* **2018**, *51*, 228-243, https://doi.org/10.1159/000495203.
66. Masui, R.; Sasaki, M.; Funaki, Y.; Ogasawara, N.; Mizuno, M.; Iida, A.; Izawa, S.; Kondo, Y.; Ito, Y.; Tamura, Y.; Yanamoto, K.; Noda, H.; Tanabe, A.; Okaniwa, N.; Yamaguchi, Y.; Iwamoto, T.; Kasugai, K. G Protein-Coupled Receptor 43 Moderates Gut Inflammation Through Cytokine Regulation from Mononuclear Cells. *Inflamm. Bowel Dis.* **2013**, *19*, 2848-2856, https://doi.org/10.1097/01.MIB.0000435444.14860.ea.
67. Zheng, X.-x.; Zhou, T.; Wang, X.-A.; Tong, X.-h.; Ding, J.-w. Histone deacetylases and atherosclerosis. *Atherosclerosis* **2015**, *240*, 355-366, https://doi.org/10.1016/j.atherosclerosis.2014.12.048.
68. Wang, L.-S.; Kuo, C.-T.; Stoner, K.; Yearsley, M.; Oshima, K.; Yu, J.; Huang, T.H.M.; Rosenberg, D.; Peiffer, D.; Stoner, G.; Huang, Y.-W. Dietary black raspberries modulate DNA methylation in dextran sodium sulfate (DSS)-induced ulcerative colitis. *Carcinogenesis* **2013**, *34*, 2842-2850, https://doi.org/10.1093/carcin/bgt310.
69. Abu-Remaileh, M.; Bender, S.; Raddatz, G.; Ansari, I.; Cohen, D.; Gutekunst, J.; Musch, T.; Linhart, H.; Breiling, A.; Pikarsky, E.; Bergman, Y.; Lyko, F. Chronic Inflammation Induces a Novel Epigenetic

Program That Is Conserved in Intestinal Adenomas and in Colorectal Cancer. *Cancer Res.* **2015**, *75*, 2120-2130, https://doi.org/10.1158/0008-5472.can-14-3295.
70. Dawood, A.E.; Manton, D.J.; Parashos, P.; Wong, R.H.; Singleton, W.; Holden, J.A.; O'Brien-Simpson, N.M.; Reynolds, E.C. Biocompatibility and Osteogenic/Calcification Potential of Casein Phosphopeptide-amorphous Calcium Phosphate Fluoride. *J. Endod.* **2018**, *44*, 452-457, https://doi.org/10.1016/j.joen.2017.11.005.
71. Kimura, I.; Ichimura, A.; Ohue-Kitano, R.; Igarashi, M. Free Fatty Acid Receptors in Health and Disease. *Physiol. Rev.* **2019**, *100*, 171-210, https://doi.org/10.1152/physrev.00041.2018.
72. Xiao, T.; Wu, S.; Yan, C.; Zhao, C.; Jin, H.; Yan, N.; Xu, J.; Wu, Y.; Li, C.; Shao, Q. Butyrate upregulates the TLR4 expression and the phosphorylation of MAPKs and NK-κB in colon cancer cell in vitro. *Oncol. Lett.* **2018**, *16*, 4439-4447, https://doi.org/10.3892/ol.2018.9201.
73. Mu, D.; Gao, Z.; Guo, H.; Zhou, G.; Sun, B. Sodium Butyrate Induces Growth Inhibition and Apoptosis in Human Prostate Cancer DU145 Cells by Up-Regulation of the Expression of Annexin A1. *PLOS ONE* **2013**, *8*, e74922, https://doi.org/10.1371/journal.pone.0074922.
74. Chriett, S.; Dąbek, A.; Wojtala, M.; Vidal, H.; Balcerczyk, A.; Pirola, L. Prominent action of butyrate over β-hydroxybutyrate as histone deacetylase inhibitor, transcriptional modulator and anti-inflammatory molecule. *Sci. Rep.* **2019**, *9*, 742, https://doi.org/10.1038/s41598-018-36941-9.
75. Finnin, M.S.; Donigian, J.R.; Cohen, A.; Richon, V.M.; Rifkind, R.A.; Marks, P.A.; Breslow, R.; Pavletich, N.P. Structures of a histone deacetylase homologue bound to the TSA and SAHA inhibitors. *Nature* **1999**, *401*, 188-193, https://doi.org/10.1038/43710.
76. Kopf, M.; Baumann, H.; Freer, G.; Freudenberg, M.; Lamers, M.; Kishimoto, T.; Zinkernagel, R.; Bluethmann, H.; Köhler, G. Impaired immune and acute-phase responses in interleukin-6-deficient mice. *Nature* **1994**, *368*, 339-342, https://doi.org/10.1038/368339a0.

Publisher's Note & Disclaimer

Supplementary materials

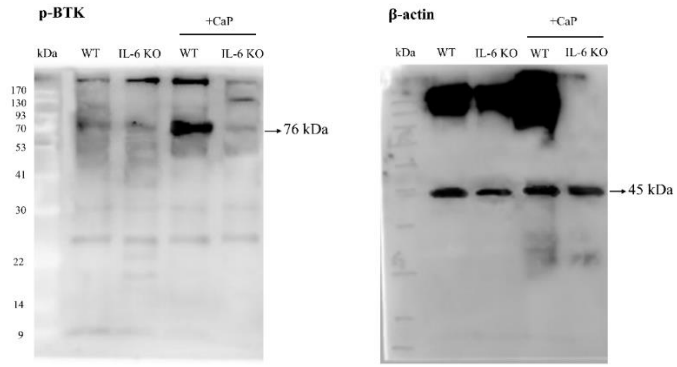

Figure S1. The full-length western blot images of Figure 1B. From left to right: Protein markers (M); the protein levels of p-BTK and β-actin in DRG of WT and IL-6 KO mice injected with/without CaP.

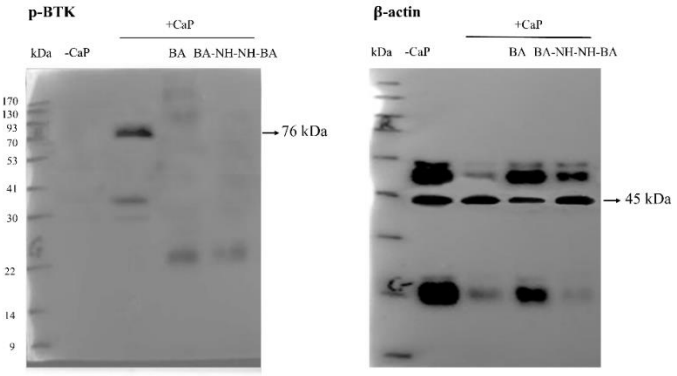

Figure S2. The full-length western blot images of Figure 2. From left to right: Protein markers (M); the protein levels of p-BTK and β-actin in DRG of CaP-injected mice and topically applied with BA or BA-NH-NH-BA.

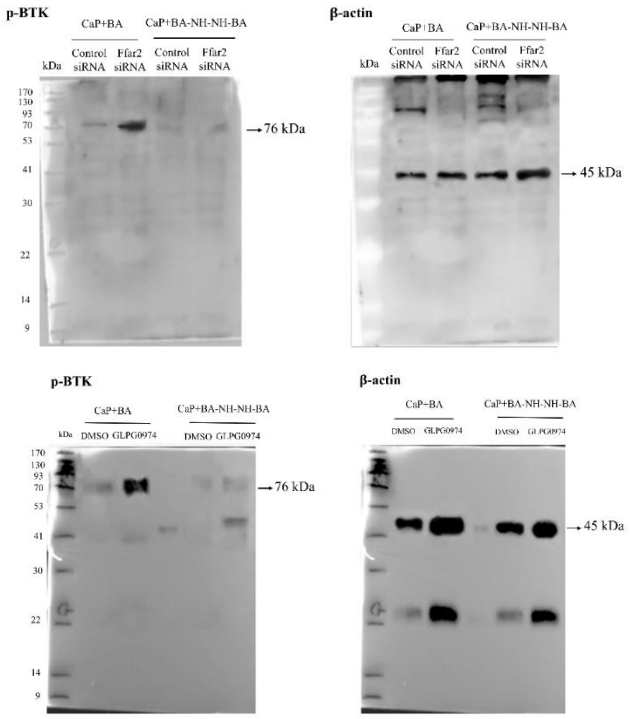

Figure S3. The full-length western blot images of Figure 4. The upper panel from left to right: Protein markers (M); the protein levels of p-BTK and β-actin in DRG of CaP-induced mice subcutaneously injection with scrambled or Ffar2 siRNA. The lower panel from left to right: gavage feeding with GLPG0974 or DMSO 10 min prior to topical application with BA or BA-NH-NH-BA.